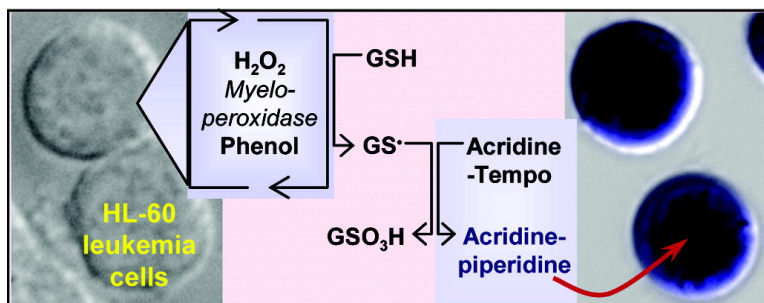


Nitroxides Scavenge Myeloperoxidase-Catalyzed Thiyl Radicals in Model Systems and in Cells

Grigory G. Borisenko, Ian Martin, Qing Zhao, Andrew A. Amoscato, and Valerian E. Kagan

J. Am. Chem. Soc., **2004**, 126 (30), 9221-9232 • DOI: 10.1021/ja0495157 • Publication Date (Web): 10 July 2004

Downloaded from <http://pubs.acs.org> on April 1, 2009



More About This Article

Additional resources and features associated with this article are available within the HTML version:

- Supporting Information
- Links to the 2 articles that cite this article, as of the time of this article download
- Access to high resolution figures
- Links to articles and content related to this article
- Copyright permission to reproduce figures and/or text from this article

[View the Full Text HTML](#)

Nitroxides Scavenge Myeloperoxidase-Catalyzed Thiyl Radicals in Model Systems and in Cells

Grigory G. Borisenko,^{*,†} Ian Martin,[†] Qing Zhao,[†] Andrew A. Amoscato,[‡] and Valerian E. Kagan^{*,†}

Contribution from the Department of Environmental and Occupational Health, University of Pittsburgh, Pittsburgh, Pennsylvania 15260, Mass Spectrometry Facility, University of Pittsburgh Center for Biotechnology and Bioengineering, Pittsburgh, Pennsylvania 15219, and Department of Pathology, University of Pittsburgh School of Medicine, Pittsburgh, Pennsylvania 15213

Received January 27, 2004; E-mail: grigoryb@yahoo.com; Kagan@pitt.edu

Abstract: Nitroxide radicals possess important antioxidant activity in live tissues because of their ability to scavenge reactive radicals. Despite the fact that, in cells, damaging free radicals are primarily quenched by glutathione (GSH) with subsequent formation of harmful glutathionyl radical (GS[•]), interactions of nitroxide radicals with GS[•] and thiols have not been studied in detail. In addition, intracellular metabolic pathways leading to the formation of secondary amines from nitroxides are unknown. Here we report that GS[•] radicals react efficiently and irreversibly with nitroxides to produce secondary amines. We developed a sensitive method for the detection of GS[•] based on their specific interaction with Ac-Tempo, a nonfluorescent conjugate of fluorogenic acridine with paramagnetic nitroxide Tempo, and used it to characterize interactions between nitroxide and thiyl radicals generated through phenoxyl radical recycling by peroxidase. During reaction of Ac-Tempo with GS[•], Tempo EPR signals decayed and acridine fluorescence concurrently increased. DMPO and PBN, spin traps for GS[•], inhibited this interaction. Using combined HPLC and mass spectrometry, we determined that 90% of the Ac-Tempo was converted into fluorescent acridine (Ac)-piperidine; GSH was primarily oxidized into sulfonic acid. In myeloperoxidase-rich HL-60 cells, Ac-piperidine fluorescence was observed upon stimulation of GS[•] generation by H₂O₂ and phenol. Development of fluorescence was prevented by preincubation of cells with the thiol-blocking reagent *N*-ethylmaleimide as well as with peroxidase inhibitors. Furthermore, Ac-Tempo preserved intracellular GSH and protected cells from phenol/GS[•] toxicity, suggesting a new mechanism for the free-radical scavenging activity of nitroxides in live cells.

Introduction

Nitroxides are stable radicals and important antioxidants that have been used to protect animal tissues from oxidative damage following cardiac arrest,¹ brain trauma,² ischemia/reperfusion,³ and γ -radiation.⁴ Their effective reactions with reactive oxygen species (ROS) such as superoxide anion radical, hydroxyl radical ([•]OH), and H₂O₂ are generally accepted to be key to the mechanisms of the nitroxide antioxidant function. However, the direct interaction of nitroxide with damaging radicals does not always provide a satisfying explanation for activities of nitroxides, such as radioprotection, which results from its reaction with secondary [•]OH-derived radicals, rather than from a direct

reaction with [•]OH formed in the course of irradiation.⁴ In addition, although secondary amines are a known major metabolite of nitroxide in cells, their origin is not clear.⁵ Furthermore, there is no identifiable biologically applicable reaction leading to the deoxygenation of nitroxide. This suggests that interactions of nitroxides studied in pure chemical systems may not be always relevant to living systems and that studies of the metabolic pathways of nitroxides in cells are required for understanding nitroxide's biological effects.

Generally, in cells, free radicals arising from toxic insults, radiation exposure, and drug metabolism are primarily scavenged by the antioxidant glutathione, whose cytosolic and mitochondrial concentrations range from 5 to 11 mM.⁶ In vitro, GSH is the major target for a wide range of free radicals, including [•]OH, RO[•], RO₂[•], and C[•]-centered radicals as well as ONOO⁻ and ¹O₂.⁷ The subsequent oxidation of GSH by these radicals results in the formation of glutathionyl radicals. While the redox potential of GS[•], H⁺/GSH is 0.9 V, it is less positive

[†] Department of Environmental and Occupational Health, University of Pittsburgh.

[‡] University of Pittsburgh Center for Biotechnology and Bioengineering and University of Pittsburgh School of Medicine.

- (1) Behringer, W.; Safar, P.; Kentner, R.; Wu, X.; Kagan, V. E.; Radovsky, A.; Clark, R. S.; Kochanek, P. M.; Subramanian, M.; Tyurin, V. A.; Tyurina, Y. Y.; Tisherman, S. A. *J. Cereb. Blood Flow Metab.* **2002**, *22*, 105.
- (2) Kwon, T. H.; Chao, D. L.; Malloy, K.; Sun, D.; Alessandri, B.; Bullock, M. R. *J. Neurotrauma* **2003**, *20*, 337.
- (3) Kato, N.; Yanaka, K.; Hyodo, K.; Homma, K.; Nagase, S.; Nose, T.; Gelvan, D. *Brain. Res.* **2003**, *979*, 188.
- (4) Samuni, A.; Goldstein, S.; Russo, A.; Mitchell, J. B.; Krishna, M. C.; Neta, P. *J. Am. Chem. Soc.* **2002**, *124*, 8719.

(5) Kroll, C.; Langner, A.; Borchert, H. H. *Free Radical Biol. Med.* **1999**, *26*, 850.

(6) Schafer, F. Q.; Buettner, G. R. *Free Radical Biol. Med.* **2001**, *30*, 1191.

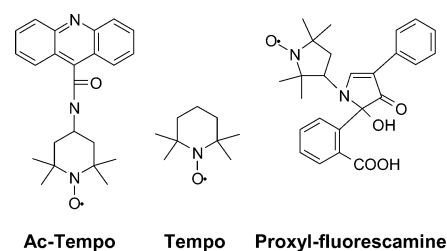
(7) Halliwell, B.; Gutteridge, J. *Free Radicals in Biology and Medicine*; Clarendon Press: Oxford, U.K., 1999.

than potentials for the above-mentioned radicals. This and extremely high GSH/GS^{*} ratio in cells explain the reason GSH is a preferred target of attack by oxidizing radicals.⁸ In cells, GS^{*} can react with glutathione anions (GS⁻) to form the glutathione disulfide anion radical (GSSG^{•-}), which reduces oxygen to superoxide radical (O₂^{•-}).⁹ Conversely, GS^{*} is a strong oxidant and can produce cell damage by reacting with protein thiols as well with unsaturated acyl chains of phospholipids in the membranes.¹⁰

This chemical cascade of free-radical propagation may represent the predominant channeling of various oxidative species by GSH within the intracellular milieu.⁸ Oxidation of GSH to GS^{*} has been shown in peroxidase-catalyzed reactions in vitro. Myeloperoxidase (MPO) and cyclooxygenase (COX), two essential inflammatory response enzymes, have been shown to generate GS^{*} in myeloperoxidase-rich HL-60 cells and COX-expressing keratinocytes, respectively.¹¹ This oxidation can be significantly enhanced during drug metabolism. Peroxidases can very efficiently oxidize phenolic compounds with intermediate formation of phenoxy radicals, which in turn promote GS^{*} production. In myeloid HL-60 cells, myeloperoxidase oxidized phenolic anticancer drug etoposide, with the formation of corresponding phenoxy radicals and consequent generation of GS^{*} and cell damage, supporting a free-radical, peroxidase-dependent mechanism for etoposide toxicity in acute myeloid leukemia.¹² It should be emphasized that GSH itself is a poor substrate for heme-containing peroxidases such as MPO and cyclooxygenase, but it is readily oxidized by non-heme GSH peroxidase. This ensures safe removal of H₂O₂ through a nonradical oxidation of GSH in cells. However, in the presence of phenols, heme-containing peroxidases will efficiently metabolize H₂O₂ with subsequent production of various radicals including phenoxy and GS^{*} radicals.

Chemical reactions of nitroxides with thiyl radicals (except thiophenols) have not been studied in detail. Because thiophenols are highly reducing compounds, nitroxides can induce oxidation of thiophenols into corresponding thiyl radicals, which, in turn, promote de-oxidation of nitroxides.¹³ In contrast to thiophenols, GSH does not reduce nitroxides. However, considering the importance of GS^{*} as a secondary radical during free-radical-mediated oxidative stress and the possible interaction of thiyl radicals with nitroxides, we proposed that the antioxidant functions of the nitroxides may involve quenching of GS^{*}. We investigated this interaction in a cell-free system, in which GS^{*} was induced by peroxidase-dependent metabolism of phenol. We also developed a new, highly sensitive method for the quantitative detection of glutathionyl radicals by electron paramagnetic resonance (EPR) and fluorescence spectroscopy.

Scheme 1. Structures of Nitroxides Examined in This Study



This method is based on the interaction of glutathionyl radicals with Ac-Tempo, a paramagnetic nonfluorescent conjugate of nitroxide and acridine 4-((9-acridinecarbonyl)amino)-2,2,6,6-tetramethylpiperidin-1-oxyl radical (Scheme 1); the interaction between Ac-Tempo and GS^{*} radicals switches off the EPR signals of the Tempo moiety and switches on the fluorescence of Ac-Tempo's acridine moiety. Through coordinated EPR and fluorescence measurements of Ac-Tempo, we observed generation of glutathionyl radicals catalyzed by purified MPO and horseradish peroxidase (HRP) in the presence of GSH and peroxidase substrates, phenol, and H₂O₂. We further applied this method to fluorescence microscopic imaging of glutathionyl radicals produced downstream of myeloperoxidase activity in HL-60 cells during phenol and H₂O₂ treatment. We found that thiyl radicals of GSH and cysteine readily react with various nitroxides and that the major products of these reactions in both our model system and in cells were corresponding sulfonic acid and secondary amine. We also were able to show that Ac-Tempo preserves cellular GSH and protects cells from phenol toxicity, thus suggesting a new mechanism for the free-radical-scavenging activity of nitroxides.

Materials and Methods

Reagents. Phenol, sodium ascorbate, 5,5-dimethyl-1-pyrroline N-oxide (DMPO), 3-amino-1,2,4-triazole, N-ethylmaleimide (NEM), α -phenyl-*tert*-butylnitron (PBN), acetonitrile (HPLC grade), diethylenetriaminepentaacetic acid (DTPA), potassium ferricyanide (K₃Fe(CN)₆), S-nitrosoglutathione (GS-NO), hydrogen peroxide (H₂O₂), succinyl acetone (SA), 2,2,6,6-tetramethylpiperidin-1-oxyl (Tempo), NADPH, glutathione, glutathione reductase (from wheat germ, EC 1.6.4.2), horseradish peroxidase (type VI, EC 1.11.1.7), superoxide dismutase (SOD), cytochrome *c* (from horse heart), and myeloperoxidase (MPO) (from human leukocytes, EC 1.11.1.7) were purchased from Sigma Chemical Co. (St. Louis, MO). 4-((9-Acridinecarbonyl)amino)-2,2,6,6-tetramethylpiperidine-1-oxyl (Ac-Tempo) and (5-(2-carboxyphenyl)-5-hydroxy-1-((2,2,5,5-tetramethyl-1-oxypyrrolidin-3-yl)methyl)-3-phenyl-2-pyrrolin-4-one) (proxyl-fluorescamine, PF) were purchased from Molecular Probes, Inc. (Eugene, OR). ThioGlo-1 reagent was purchased from Covalent Associates, Inc. (Woburn, MA). Fetal bovine serum was purchased from Sigma Chemical Co. (St. Louis, MO).

Peroxidase-Catalyzed Generation of Glutathionyl Radicals in Model System. Peroxidase-catalyzed reactions were studied using a system comprising GSH, phenol, H₂O₂, and peroxidase (MPO or HRP). In this system, catalytic cycling of peroxidase is described by two-electron reduction of hydrogen peroxide into water and two-electron oxidation of heme iron at catalytic site (so-called compound I). Then compound I catalyzed one-electron oxidation of two phenol molecules into phenoxy radicals, and thus catalytic site returned into native state. Phenoxy radicals recycled back to phenol through the oxidation of GSH to thiyl radicals.^{11a,12} Unlike phenol, GSH itself is a poor substrate for peroxidases; generation of glutathionyl radicals in the absence of phenolic compounds is very low. Production of glutathionyl radicals

- (8) Buettner, G. R. *Arch. Biochem. Biophys.* **1993**, *300*, 535.
 (9) (a) Koppenol, W. H. *Free Radical Biol. Med.* **1993**, *14*, 91. (b) Winterbourn, C. C. *Free Radical Biol. Med.* **1993**, *14*, 85.
 (10) Schoneich, C.; Dillinger, U.; Von Bruchhausen, F.; Asmus, K. D. *Arch. Biochem. Biophys.* **1992**, *292*, 456.
 (11) (a) Ross, D.; Albano, E.; Nilsson, U.; Moldeus, P. *Biochem. Biophys. Res. Commun.* **1984**, *125*, 109. (b) Schreiber, J.; Foureman, G. L.; Hughes, M. F.; Mason, R. P.; Eling, T. E. *J. Biol. Chem.* **1989**, *264*, 7936. (c) Stoyanovsky, D. A.; Goldman, R.; Jonnalagadda, S. S.; Day, B. W.; Claycamp, H. G.; Kagan, V. E. *Arch. Biochem. Biophys.* **1996**, *330*, 3.
 (12) Kagan, V. E.; Yalowich, J. C.; Borisenko, G. G.; Tyurina, Y. Y.; Tyurin, V. A.; Thampatty, P.; Fabisiaik, J. P. *Mol. Pharmacol.* **1999**, *56*, 494.
 (13) (a) Murayama, K.; Yoshioka T. *Bull. Chem. Soc. Jpn.* **1969**, *42*, 2, 1942. (b) Carloni, P.; Damiani, E.; Iacussi, M.; Greci, L.; Stipa, P.; Cauzi, D.; Rizzoli, C.; Sgarabotto, P. *Tetrahedron* **1995**, *51*, 12445. (c) Damiani, E.; Carloni, P.; Iacussi, M.; Stipa, P.; Greci, L. *Eur. J. Org. Chem.* **1999**, *9*, 2405.

in peroxidase-catalyzed reaction was tested with spin traps, DMPO and PBN, that form stable adducts with glutathionyl radical (DMPO/glutathionyl (DMPO/GS[•]) and PBN/GS[•], respectively).

Photolysis of S-Nitrosoglutathione. According to previous reports, near-UV light induces homolytic cleavage of S–N bond of GS–NO with concomitant formation of GS[•] and nitric oxide (NO).¹⁴ An Oriol UV light source (model 66002; Oriol Instruments, Stratford, CT) with wavelength range of 300–700 nm and bulb power at 100 W was used to decompose GS–NO (0–20 μ M). Samples were irradiated in the presence of Ac-Tempo (10 μ M), DMPO (100 mM), or both for 2 min at a 10-cm distance from the source.

Cells and Cell Culture. The human leukemia HL-60 cell line was grown in RPMI 1640 medium supplemented with 12% fetal bovine serum at 37 °C under 5% CO₂ atmosphere. Cell viability was assessed using Trypan Blue dye exclusion in cell suspensions (5×10^5 cells/mL). To deplete myeloperoxidase activity, the myeloperoxidase-rich cells were treated with 0.4 mM SA for 72 h. Myeloperoxidase activity in cells was monitored on a Shimadzu UV160U spectrophotometer using guaiacol assay as described previously.¹² To block reactions of low molecular weight thiols, cells were pretreated with NEM at relatively low concentration of 50 μ M for a short period of time (5 min), which preferentially depletes GSH and free cysteine.

Fluorescence Spectroscopy. Ac-Tempo. Concentration of Ac-Tempo was determined by measurements of optical density at 359 nm ($\epsilon = 10.4 \text{ mM}^{-1} \text{ cm}^{-1}$) using a Shimadzu UV160U spectrophotometer. For measurements of Ac-Tempo fluorescence, a Shimadzu spectrofluorimeter RF-5301PC set at an excitation wavelength 361 nm, an excitation slit of 1.5 nm, and an emission slit of 3 nm was used. Time courses of fluorescence intensity were detected using an emission wavelength 440 nm. The amount of fluorescent product formed from Ac-Tempo in HL-60 cells was estimated on the basis of calibration curves obtained by complete conversion of Ac-Tempo into its fluorescent derivative Ac-piperidine by a cell-free, purified peroxidase system. Cells treated with Ac-Tempo were centrifuged once (1000g, 5 min), and their pellet was resuspended in equal volume of PBS prior to taking the measurements.

Proxyl Fluorescamine. Proxyl-fluorescamine is a pyrrolidin-derived nitroxide with physicochemical properties analogous to Ac-Tempo. The time course of PF fluorescence was monitored using excitation and emission wavelengths of 385 and 485 nm, respectively, and excitation and emission slits of 3 and 10 nm, respectively.

GSH. GSH content was determined using ThioGlo-1 reagent, a maleimide reagent that forms a highly fluorescent product upon reaction with SH groups.¹⁵ In cell-free model system with purified peroxidase, GSH content was estimated by an immediate fluorescence response registered on addition of sample to the ThioGlo-1 reagent. In cells, GSH content was determined in similar manner: cells were centrifuged at 1000g for 5 min, and the pellet was resuspended in PBS and then homogenized by freezing and thawing. Protein SH groups were determined as an additional fluorescent response induced by treatment of samples with 4 mM SDS to unfold proteins. Lack of interference of Ac-Tempo with the ThioGlo assay was verified in separate experiments with the model system and in vitro.

Glutathione Disulfide. Glutathione disulfide content was detected as an additional fluorescence response after addition of NADPH (0.5 mM) and glutathione reductase (1 U/mL) to the same sample. The spectrofluorimeter was set at 1.5 and 3 nm for excitation and emission slits, respectively, and 388 and 500 nm for excitation and emission wavelengths, respectively.

EPR Spectroscopy. EPR measurements were performed on a JEOL-RE1X spectrometer at 25 °C in glass capillary tubes (1.2 mm i.d.)

obtained from Fischer Scientific Co. (Pittsburgh, PA). The tube was filled with 50 μ L of sample and placed in an opened, 3.0 mm i.d. EPR quartz tube. Ac-Tempo, Tempo, and PF EPR spectra were recorded under the following conditions: 335.7 mT, center field; 8 mT, sweep width; 0.32 mT, field modulation; 10 mW, microwave power; 0.1 s, time constant; 1 min, time scan. Spectra of DMPO/GS[•] were recorded under the same conditions, except field modulation was adjusted to 0.2 mT. The time course of Ac-Tempo EPR signals was obtained by repeated scanning of the field corresponding to a middle peak of the EPR spectrum under the following instrumental conditions: 335.5 mT, center field; 0.8 mT, sweep width; 0.32 mT, field modulation; 10 mW, microwave power; 0.1 s, time constant; 10 s, time scan; internal mode of recording. The time course of PF EPR signals was recorded under the same conditions, with the exception of a center field adjustment to 335.3 mT.

Detection of Ac-Tempo Derivatives. HPLC Analysis. HPLC analysis was performed on a Shimadzu LC-600 liquid chromatograph equipped with a Shimadzu RF-551 fluorescent detector, a Shimadzu SPD-M10A absorbance diode-array detector, or a JEOL-RE1X EPR spectrometer. The sample was applied to a reverse-phase Beckman C₁₈ UI-transphere ODS column (5 μ m, 4.5 \times 250 mm) equilibrated with a solvent A (75 mM ammonium acetate, 50 mM citric acid, 10% acetonitrile, pH 3.0). The column was eluted for 15 min with a linear gradient (from 0 to 30%) of solvent B (100% acetonitrile). The flow rate was 1 mL/min, and the injection volume was 20 μ L. The eluent was monitored by optical density in the range of 200–400 nm by Ac-Tempo fluorescence using an excitation wavelength of 361 nm and emission wavelength of 440 nm and by Ac-Tempo EPR signal obtained by repeated scanning of the field corresponding to a middle peak of the EPR spectrum under the conditions described above.

Mass Spectrometry. Ac-Tempo, GSH, and their reaction products were analyzed by electrospray ionization mass spectrometry through direct infusion into a Quattro II, triple quadrupole mass spectrometer (Micromass, Inc., Manchester, England). The electrospray probe was operated at a voltage differential of 3.5 keV (positive ion mode). Mass spectra were obtained by scanning the range of 150–950 m/z every 2.6 s and summing individual spectra. Source temperature was maintained at 70 °C. Collision-induced decomposition (CID) tandem mass spectra were obtained by selecting the ion of interest and performing daughter-ion scanning in Q3 using argon gas in the collision chamber. The spectrometer was operated at unit resolution in Q1 and slightly below unit resolution in Q3.

Detection of GS[•] in HL-60 Cells Using Fluorescence Microscopy. Cells were preincubated with Ac-Tempo (20 μ M) in PBS for 5 min. Phenol (100 μ M) and H₂O₂ (20 μ M) were then added for another 5-min incubation. After the treatments, cells were centrifuged at 1000g for 5 min and resuspended in PBS. Glutathionyl radical formation in cells was evaluated by Ac-Tempo fluorescence analysis using a Nikon ECLIPSE TE 200 fluorescence microscope (Tokyo, Japan) equipped with a digital Hamamatsu CCD camera (C4742-95-12NRB). At least 200 cells per experimental condition were counted.

Data Analysis. Data are expressed as means \pm SD. Changes in variables for different assays were analyzed by either Student's *t* test (single comparisons) or one-way ANOVA for multiple comparisons. Differences among means were considered to be significant at $p < 0.05$.

Reaction rate of GS[•] with Ac-Tempo was approximated on the basis of the results of competition experiments with DMPO. The rate was also approximated by computer simulation of Ac-Tempo fluorescence production, which was carried out by numerical integration using Visual Basic. Rate constants of GS[•] reactions with O₂ and GS⁻ were obtained from the literature.^{9b,16} The rate of GSH oxidation was estimated using the ThioGlo assay as described above. Finally, kinetics of fluorescence production were analyzed by a least-squares fitting to the system of reaction equations with GS[•]/Ac-Tempo rate varied to obtain the best fit employing interval methods for global optimization.

(14) Stamler, J. S.; Jaraki, O.; Osborne, J.; Simon, D. I.; Keane, J.; Vita, J.; Singel, D.; Valeri, C. R.; Loscalzo, J. *Proc. Natl. Acad. Sci. U.S.A.* **1992**, *89*, 7674.

(15) Langmuir, M. E.; Yang, J.-R.; LeCompte, K. A.; Durand, R. E. In *Fluorescence Microscopy and Fluorescent Probes*; Slavik, J., Ed.; Plenum Press: New York, 1996; pp 229–234.

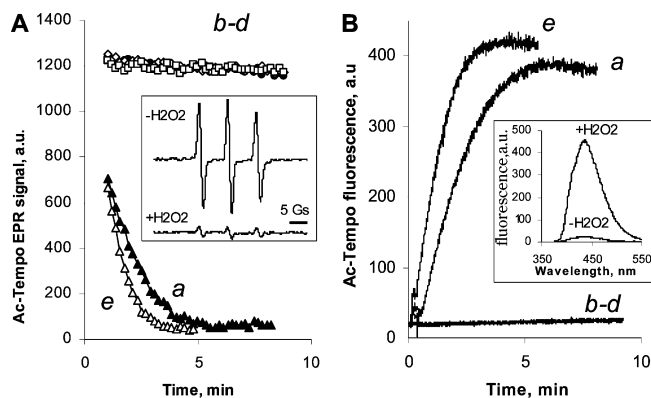


Figure 1. Time course of Ac-Tempo EPR signal decay and fluorescence production catalyzed by MPO and HRP in model systems. (A) Time course of Ac-Tempo EPR signals was obtained by repeated scanning of the field corresponding to a middle peak of the EPR spectrum under the following instrumental conditions: 335.5 mT, center field; 0.4 mT, sweep width; 0.2 mT, field modulation; 10 mW, microwave power; 0.1 s, time constant; 10 s, time scan; internal mode of recording. Insert: EPR spectra of Ac-Tempo after incubation with MPO/phenol/GSH in the presence or in the absence of H_2O_2 during 5 min. (B) Time course of fluorescence was detected using excitation and emission wavelengths of 361 and 440 nm, respectively. Insert: Fluorescence spectra of Ac-Tempo were obtained in the same incubation conditions as EPR spectra. Incubation conditions for both panels: (a) (\blacktriangle) 0.2 U/mL of MPO, 10 μM Ac-Tempo, 50 μM phenol, 10 μM GSH, 10 μM H_2O_2 ; (b) (\square) same as that in (a), but minus phenol; (c) (\diamond) same as that in (a), but minus H_2O_2 ; (d) (\bullet) same as that in (a), but minus GSH; (e) (Δ) same as that in (a), but with 0.2 U/mL of HRP instead of MPO. EPR and fluorescence spectra and time course traces are representative recordings obtained from more than 30 experiments.

Results

Peroxidases Catalyze GSH-Dependent Ac-Tempo Modification.

The Ac-Tempo conjugate contains two moieties: hydrophobic fluorogenic acridine and paramagnetic Tempo, a stable nitroxide radical with unpaired electron located on the N–O group (Scheme 1). The conjugate also retains paramagnetic properties; however, this conjugate loses its fluorescent properties because of quenching produced by electron exchange interactions between the Tempo radical and the excited state of acridine.¹⁷ Chemical modification of the nitroxide moiety can trigger disappearance of the EPR signal and restore fluorescence of Ac-Tempo. Therefore, modifications of the molecule can be detected by EPR and fluorescence spectroscopy. Ac-Tempo shows a characteristic triplet EPR signal with hyperfine constant $a_{\text{Tempo}}^{\text{N}} = 16.9$ G (Figure 1A, insert). Decay of the Ac-Tempo EPR signal was observed in the presence of our cell-free thyl radical-generating system (Figure 1A). In this system, glutathionyl radicals were produced through recycling of phenoxyl radicals, which were catalytically generated by peroxidase/ H_2O_2 system (see Materials and Methods section for further explanations). Fluorescence from acridine grew in synchrony with the decay of EPR signals (Figure 1B). Only negligible changes in EPR signal or fluorescence response were detected in the absence of GSH, MPO, or phenol in the reaction mixture, suggesting that Ac-Tempo was not modified directly by MPO or by phenoxyl radicals produced in this system. Similar

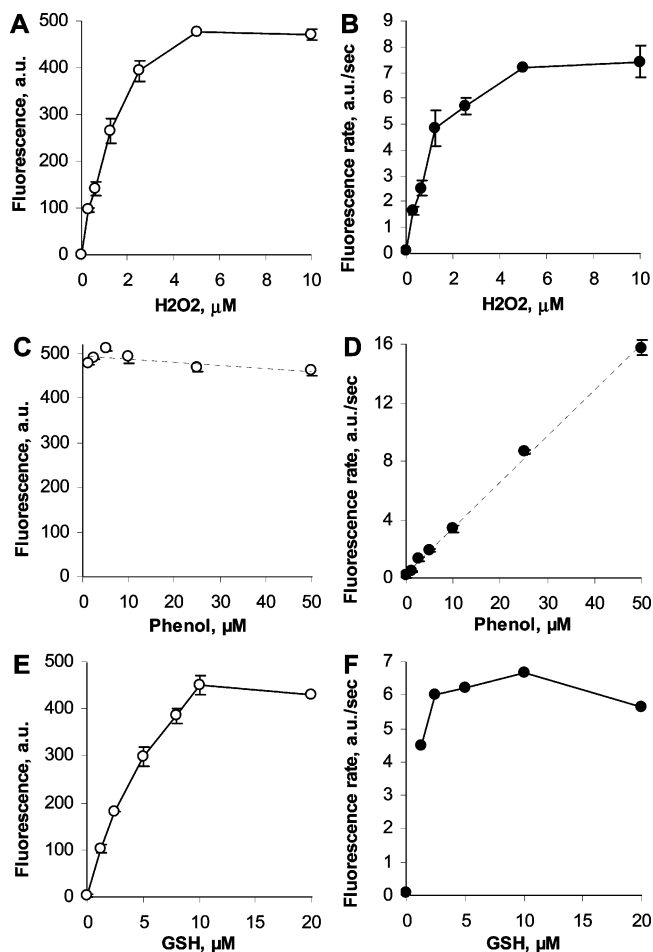


Figure 2. Dependence of rate and yield of Ac-Tempo fluorescence production on H_2O_2 , phenol, and GSH concentrations. Total fluorescence yield at the end of reaction (A, C, E) and initial rate of fluorescence generation (B, D, F) after incubation with GSH, H_2O_2 , and/or phenol. Instrumental conditions were the same as those noted in Figure 1. Note that fluorescence of 500 au corresponds to nearly total transformation of Ac-Tempo into its fluorescent derivative. Incubation conditions: (A, B) 10 μM GSH, 50 μM phenol; (C, D) 10 μM GSH, 10 μM H_2O_2 ; (E, F) 10 μM H_2O_2 , 50 μM phenol. Ac-Tempo (10 μM) and HRP (0.2 U/mL) were used in all experiments. Data represent means \pm SD ($n = 4$).

observations were made by EPR and fluorescence spectroscopy when MPO was replaced by HRP. Glutathione did not react directly with nitroxide and did not induce observable changes in EPR or fluorescence signals even at high concentrations (up to 5 mM, data not shown).

H_2O_2 concentration governed total yield of fluorescence intensity (Figure 2A). Analogous observations were made over a range of GSH concentrations: a linear correlation was observed between the amount of GSH added and final fluorescence intensity until nearly complete transformation of Ac-Tempo (Figure 2E). Stoichiometry of GSH and Ac-Tempo consumption was nearly 1:1 as determined by measurements of Ac-Tempo fluorescence production paralleled by measurements of GSH utilization using the ThioGlo-1 assay (data not shown). In contrast to H_2O_2 and GSH, changes in phenol concentration did not affect total reaction yield (Figure 2C). Relatively low phenol concentrations (~ 1 μM) were sufficient to convert substantially higher concentrations of Ac-Tempo (10 μM) to its fluorescent product in the presence of excessive amounts of GSH and H_2O_2 . This supports the view that phenol

(16) (a) Monig, J.; Asmus, K. D.; Forni, L. G.; Willson, R. L. *Int. J. Radiat. Biol. Relat. Stud. Phys., Chem. Med.* **1987**, *52*, 589. (b) Grierson, L.; Hildenbrand, K.; Bothe, E. *Int. J. Radiat. Biol.* **1992**, *62*, 265. (c) Tamba, M.; Simone, G.; Quintiliani, M. *Int. J. Radiat. Biol. Relat. Stud. Phys., Chem. Med.* **1986**, *50*, 595. (d) Winterbourn, C. C.; Metodiewa, D. *Free Radical Biol. Med.* **1999**, *27*, 322.

(17) Herbelin, S. E.; Blough, N. V. *J. Phys. Chem. B* **1998**, *102*, 8170.

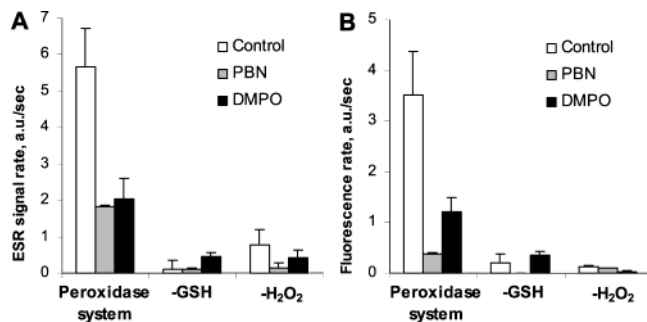


Figure 3. Effects of DMPO and PBN on the rates of Ac-Tempo EPR signal decay and fluorescence production catalyzed by HRP in the model system. Rates of Ac-Tempo EPR signal (A) or fluorescence intensity (B) were measured in the presence of combinations of HRP/phenol/GSH/H₂O₂ (control, open bars) and 100 mM PBN (gray bars) or 100 mM DMPO (black bars). Other incubation conditions: Peroxidase system: 0.2 U/mL of HRP, 10 μ M Ac-Tempo, 50 μ M phenol, 10 μ M GSH, 10 μ M H₂O₂; plus spin trap; -GSH: same as peroxidase system, but minus GSH; -H₂O₂: same as peroxidase system, but minus H₂O₂. Instrumental conditions were the same as those in Figure 1. Data represent means \pm SD ($n = 3$).

is recycled in this system. The rate of the reaction was strongly dependent on H₂O₂ and phenol concentrations (substrates for peroxidase) but not on GSH concentration (not a good substrate for peroxidases) (Figure 2B,D,F), suggesting that Ac-Tempo modification was completely dependent on the peroxidase activity associated with GSH oxidation.

Glutathionyl Radical Initiates Ac-Tempo Modification.

Spin traps, DMPO and PBN, inhibited decay of Ac-Tempo EPR signals and generation of fluorescence in the presence of HRP/phenol/GSH/H₂O₂ (Figure 3A,B). DMPO/GS[•] or PBN/GS[•] formation was not detected by EPR under these experimental conditions in either the presence or the absence of Ac-Tempo because of peroxidase-catalyzed metabolism and instability of these adducts.¹⁸ However, their observation became possible upon addition of 10 times higher amounts of H₂O₂ and GSH (data not shown).

Generation of Glutathionyl Radicals Using Photolysis of GS-NO. To obtain independent evidence for a direct reaction between Ac-Tempo and GS[•], the latter radical was generated using photolysis of S-nitrosylated glutathione (GS-NO). During irradiation of GS-NO in the presence of DMPO, an EPR signal was detected with splitting constants $a^N = 15.4$ G, $a^{H\beta} = 16.2$ G, characteristic of the DMPO/GS[•] adduct (Figure 4B, marked with tick). In control experiments, irradiation of Ac-Tempo alone and with GSH, or incubation of Ac-Tempo with an NO donor, PAPANONOate, in the dark, did not affect the nitroxide EPR signal or induced fluorescence. Irradiation of GS-NO in the presence of Ac-Tempo caused depletion of the nitroxide EPR signal and appearance of the fluorescent product (Figure 4A, columns 3 and 4). Both methods showed that the reaction yield depended on the amount of GS-NO that decomposed. Furthermore, both methods showed that addition of an excess of DMPO blocked the reaction (note that the DMPO vs Ac-Tempo ratio was 10 000:1) (Figure 4A,B), suggesting a direct reaction between Ac-Tempo and GS[•].

To test whether Ac-Tempo could compete with DPMO for GS[•], we increased the concentration of Ac-Tempo in the system containing DMPO and GS-NO. When the higher Ac-Tempo concentration was used, a lower EPR signal of DMPO/GS[•]

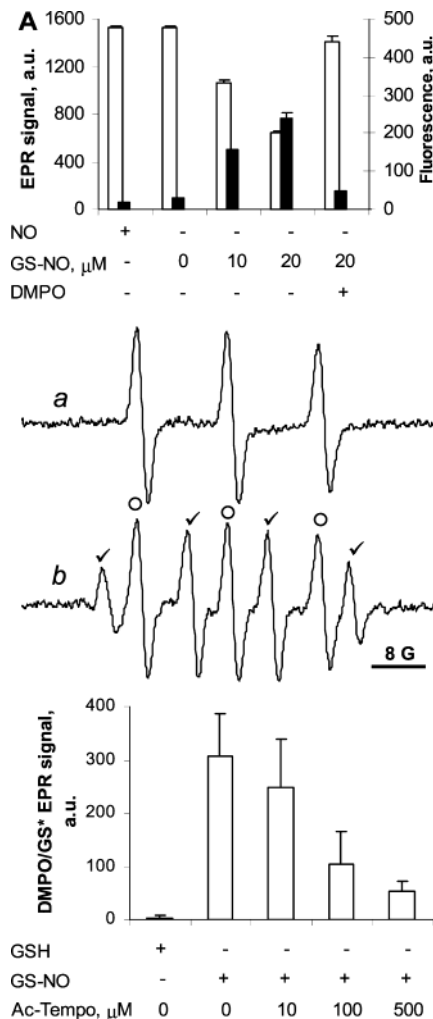


Figure 4. EPR spectra of Ac-Tempo and fluorescence production during reaction with glutathionyl radicals produced by photolysis of GS-NO. Effects of DMPO. (A) Ac-Tempo (10 μ M) was incubated with 0.2 mM PAPANONOate (NO), 0, 10, 20 μ M GS-NO (GS-NO), or 20 μ M GS-NO and 100 mM DMPO (DMPO). Mixtures containing GS-NO were irradiated with UV/vis light. EPR spectra intensity (open bars) and fluorescence intensity (closed bars) were obtained as described in Figure 1. Whole scales of EPR and fluorescence intensities represent approximately the same amounts of Ac-Tempo and its fluorescent product, respectively. (B) EPR spectra recorded from the solution of 10 μ M Ac-Tempo, 100 mM DMPO, and 20 μ M GS-NO before (a) and after (b) irradiation. EPR spectrum of Ac-Tempo is marked with O; the spectrum of DMPO/GS[•] adduct is marked with a tick. Conditions for EPR spectroscopy were: 335.5 mT, center field; 8 mT, sweep width; 0.2 mT, field modulation; 10 mW, microwave power; 0.1 s, time constant; 1 min, time scan. (C) Effect of various Ac-Tempo concentrations on the DMPO/GS[•] adduct formation. Instrumental and incubation conditions are same as in (B). Data represent means \pm SD ($n = 4$).

adduct was observed. It was diminished 2-fold at Ac-Tempo concentration of 0.1 mM (DMPO/Ac-Tempo ratio 1000:1; Figure 4C), suggesting that Ac-Tempo is more reactive toward GS[•] than DMPO by 2 to 3 orders of magnitude.

Interaction of Ac-Tempo with Glutathione Disulfide Anion Radical and Superoxide Radicals. GS[•] can initiate several secondary reactions with GS⁻ and O₂ yielding GSSG⁻ and O₂⁻, which might also react with Ac-Tempo and reduce it to EPR silent and fluorescent hydroxylamine. To test this possibility, we increased GSH levels, creating favorable conditions for GSSG⁻ formation. Lower rates of H₂O₂-dependent fluorescence production were observed in the presence of 10 μ M

(18) Mao, G. D.; Thomas, P. D.; Poznansky, M. J. *Free Radical Biol. Med.* 1994, 16, 493.

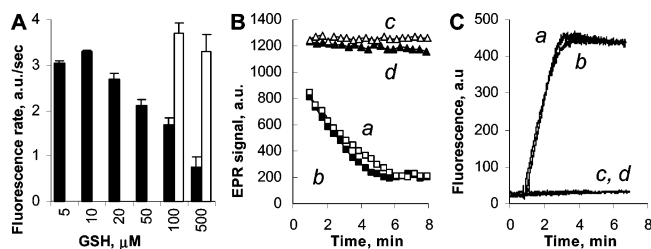


Figure 5. Effects of SOD and GSH on the Ac-Tempo EPR signal decay and fluorescence production catalyzed by HRP. (A) Effect of high GSH concentrations on the fluorescence production rate in the Ac-Tempo/HRP/phenol/GSH/H₂O₂ system (open bars: 10 μ M Ac-Tempo; filled bars: 50 μ M Ac-Tempo). (B, C) Ac-Tempo EPR signal and fluorescence production from peroxidase system, respectively. (a) (\square) 10 μ M Ac-Tempo, 0.2 U/mL of HRP, 50 μ M phenol, 10 μ M H₂O₂, 10 μ M GSH. (b) (\blacksquare) Same as (a), plus 100 U/mL of SOD. (c) (Δ) Same as (a), minus H₂O₂. (d) (\blacktriangle) Same as (c), plus SOD. Instrumental conditions were the same as those in Figure 4. Data represent means \pm SD ($n = 4$).

Ac-Tempo (Figure 5A); reaction was almost completely blocked at 1 mM GSH (data not shown). This suggests that GSH surpassed Ac-Tempo in reactions with glutathionyl radicals, but GSSG^{•-} radicals had no significant impact on Ac-Tempo modification. Indeed, rates of fluorescence production were increased when 50 μ M Ac-Tempo was added to the incubation system containing high GSH concentrations (Figure 5A).

Ac-Tempo EPR signal decay and production of fluorescence were not affected by addition of SOD to the peroxidase-catalyzed reaction (Figure 5B,C). It is important to note that as little as 10 U/mL of SOD was enough to completely dismutate all O₂^{•-} that could possibly be formed in a system with peroxidase/H₂O₂/phenol/GSH, as we have found by a cytochrome *c* reduction assay in the presence of xanthine/xanthine oxidase (data not shown). However, SOD concentrations up to 100 U/mL in our system had no effect on either rate or yield of Ac-Tempo modification by peroxidase (Figure 5B,C).

The superoxide-generating xanthine/xanthine oxidase system, adjusted to produce \sim 2 nmol O₂^{•-}/min, did not alter the physical properties of Ac-Tempo as revealed by EPR and fluorescence spectroscopy (data not shown).

Interaction of Ac-Tempo with Cysteine and Tempo and Proxyl-Fluorescamine with GSH. Substitution of cysteine for GSH in peroxidase system did not produce significant difference in the fluorescence emission from Ac-Tempo. Quick development of fluorescence was detected in the incubation system comprising HRP/Cys/phenol and H₂O₂; in the absence of either phenol or H₂O₂ or HRP, the fluorescence response was significantly lower or did not develop at all (data not shown).

Two other nitroxides were tested for the reactivity toward glutathionyl radicals. When Tempo was utilized in the peroxidase system, its EPR signal decayed at a similar rate as was observed for Ac-Tempo (data not shown). PF, pyrrolidin-derived nitroxide with physicochemical properties analogous to Ac-Tempo (Scheme 1), which was previously applied for the fluorescent detection of \cdot OH and O₂^{•-},¹⁹ appeared to be highly sensitive to light and thus generated nonspecific fluorescence. However, by using a short exposure time and by constantly mixing the sample, we were able to obtain results consistent with those for Ac-Tempo. Similar to Ac-Tempo, the rate of PF

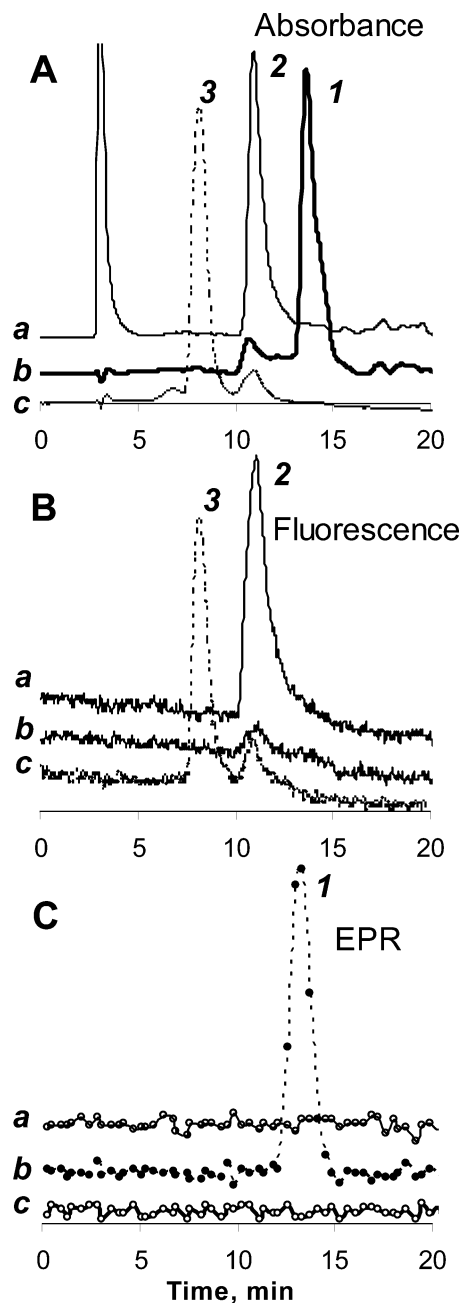


Figure 6. HPLC profiles of Ac-Tempo and its derivatives. HPLC profiles of Ac-Tempo and its derivatives were detected using an optical diode-array detector (A), a fluorescence detector (B), or an EPR spectrometer (C). Sample preparation: (a) Ac-Tempo-H, obtained by reduction of Ac-Tempo (130 μ M) with ascorbate (650 μ M) for 15 min; (b) Ac-Tempo standard (130 μ M); (c) same as (b), plus 0.3 U/mL of HRP, 50 μ M phenol, 130 μ M H₂O₂, and 200 μ M GSH, incubation time 10 min. HPLC profiles are representative of at least five experiments.

fluorescence production in the presence of HRP/GSH/phenol and H₂O₂ was dramatically higher than rates produced when one of the components was omitted. The EPR signal from PF decayed concomitantly with the fluorescence increase (data not shown).

HPLC Detection and MS Analysis of Ac-Tempo Products. HPLC conditions were adjusted to separate Ac-Tempo and its derivatives. Using UV-vis detector, we found that standard Ac-Tempo eluted with a retention time (t_R) of 14 min (Figure 6A, peak 1), hydroxylamine of Ac-Tempo (Ac-Tempo-H) prepared by reduction with ascorbate had $t_R = 11$ min (peak 2), and the

(19) (a) Blough, N. V.; Simpson, D. J. *J. Am. Chem. Soc.* **1988**, *110*, 1915. (b) Pou, S.; Huang, Y. L.; Bhan, A.; Bhadti, V. S.; Hosmane, R. S.; Wu, S. Y.; Cao, G. L.; Rosen, G. M. *Anal. Biochem.* **1993**, *212*, 85.

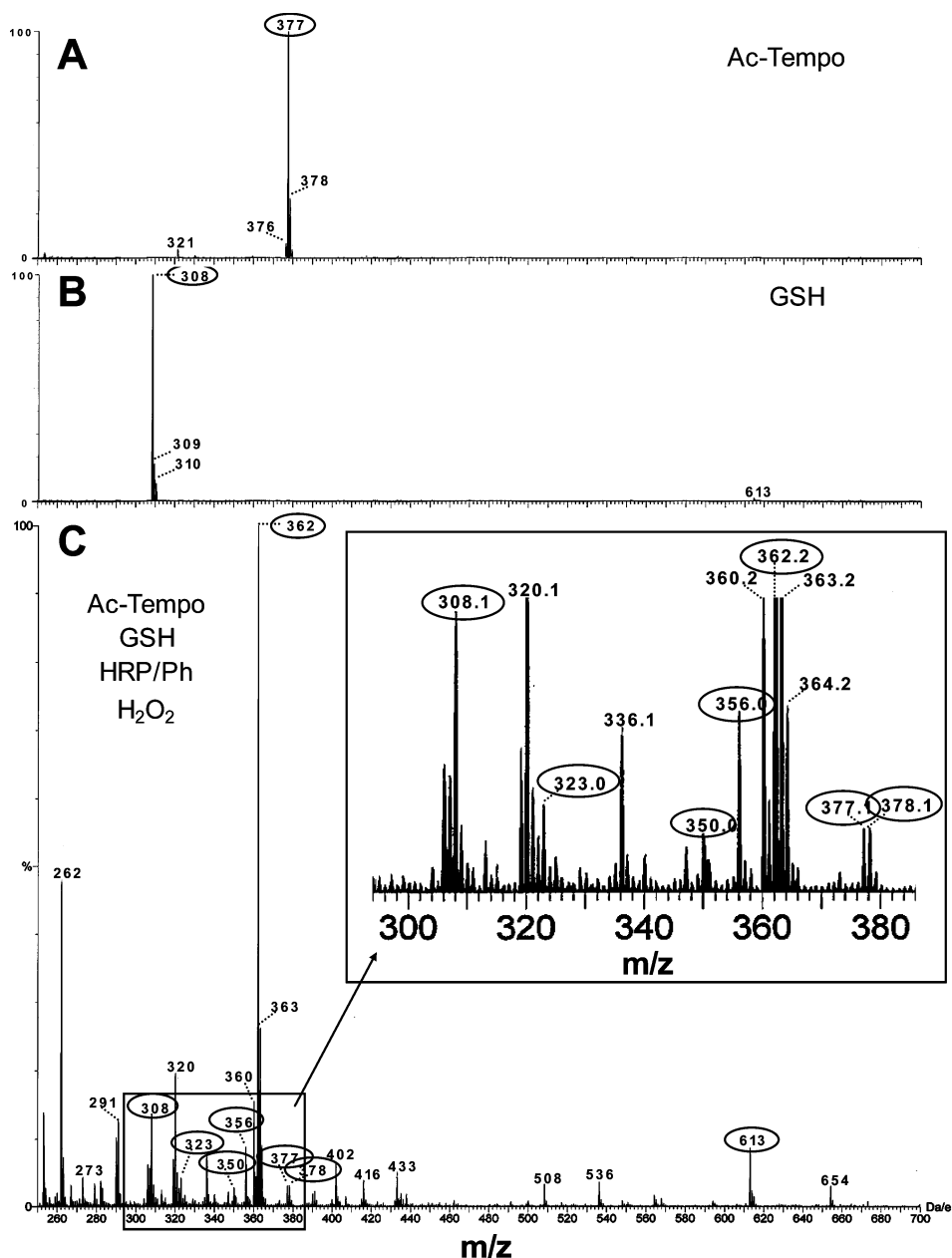


Figure 7. Mass spectra of Ac-Tempo and GSH after incubation with complete peroxidase system. (A) MS spectrum of Ac-Tempo standard with m/z 377. (B) MS spectrum of GSH standard with m/z 308. (C) MS spectrum of complete HRP-containing system. Incubation conditions: 100 μM Ac-Tempo, 200 μM GSH, 0.2 U/mL of HRP, 50 μM phenol, 10 μM H_2O_2 , ammonium acetate buffer pH 6.0. Inset: Magnification of the part of the spectrum containing peaks of GSH, Ac-Tempo, and their derivatives. The peak at m/z 378 represents hydroxylamine of Ac-Tempo; at m/z 362 it represents Ac-piperidine; at m/z 350 it represents Ac-Tempo-glutathione sulfoxide; at m/z 307 and 613 it represents GSSG; at m/z 323 it represents GSOH; and at m/z 356 it represents GSO_3H .

major product of Ac-Tempo oxidation by the peroxidase/ H_2O_2 /phenol/GSH system had $t_{\text{R}} = 8$ min (peak 3). All three HPLC peaks had similar absorbance spectra corresponding to Ac-Tempo. However, only Ac-Tempo-H and its oxidation product were fluorescent (Figure 6B, peaks 2 and 3), and only Ac-Tempo was detectable by EPR spectroscopy (Figure 6C, peak 1).

Mass spectrometry analysis showed that Ac-Tempo (m/z 377) was predominantly converted to the compound with m/z 362, which is consistent with $[\text{M} - \text{O}]^+$ of 4-((9-acridinecarbonyl)-amino)-2,2,6,6-tetramethylpiperidine (Ac-piperidine) (Figure 7). A minor fraction of Ac-Tempo was converted to the compound with m/z 378 that corresponded to Ac-Tempo-H. The identity of these compounds was unambiguously supported by the structural analysis using CID tandem MS, which revealed

comparable fragmentation spectra for compounds with m/z 377 and 362 compatible with Ac-Tempo and Ac-piperidine structures, respectively (Figure 8A,B). In addition to Ac-piperidine and Ac-Tempo-H, we were able to detect trace amounts of the doubly charged ion with m/z 350, the $[\text{M} + 2\text{H}]^{2+}$ of the compound with $M_{\text{r}} = 698$, a probable Ac-Tempo-glutathione sulfoxide (Figure 7). Indeed, according to MS/MS analysis, this compound was likely to be Ac-Tempo-glutathione sulfoxide (Figure 8C). Thus, two main products of peroxidase-catalyzed reactions, Ac-piperidine (85–90%) and Ac-Tempo-H (~10–15%), were identified by combined HPLC and MS analysis. In accordance with these data, treatment of the end products of peroxidase reaction with ferricyanide, which could oxidize hydroxylamine back to nitroxide, revealed a recovery of the

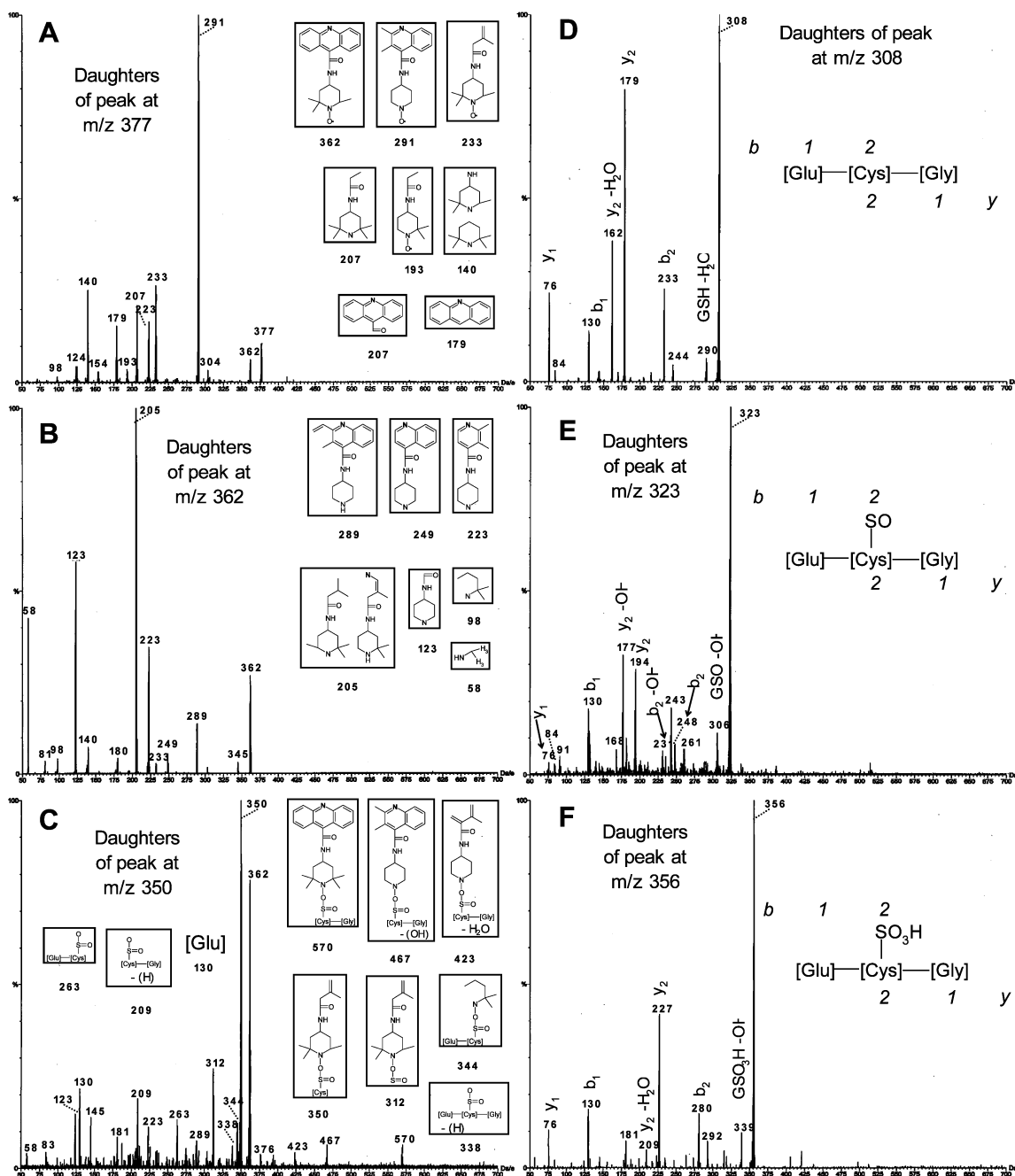


Figure 8. Collision-induced decomposition spectra of Ac-Tempo, GSH, and their derivatives formed during peroxidase-catalyzed reaction. (A) CID spectrum of m/z 377, Ac-Tempo. (B) CID spectrum of m/z 362, Ac-piperidine. (C) CID spectrum of m/z 350, the $[M + 2H]^{2+}$ of the Ac-Tempo-glutathione sulfoxide. (D) CID spectrum of m/z 308, GSH. (E) CID spectrum of m/z 323, GSOH. (F) CID spectrum of m/z 356, GSO₃H. Structural formulas in inserts represent fragments corresponding to the peaks on CID spectra. Note that several structures drawn on (A) or (B) correspond to similar peaks on both panels.

original EPR signal by $\sim 15\%$ that was paralleled by quenching of fluorescence by $\sim 15\%$ (data not shown).

Glutathione Consumption during Peroxidase-Catalyzed Oxidation of GSH in the Presence of Ac-Tempo. As determined by fluorescence ThioGlo-1 assay, 97% of GSH was oxidized by the peroxidase-catalyzed reaction when H₂O₂ was added in excess (data not shown). However, less than 20% of GSH was converted to GSSG in the presence of Ac-Tempo; the major part of GSH was irreversibly oxidized. It is interesting to note that Ac-Tempo was reduced to hydroxylamine during this reaction also by 10–15%.

MS analysis of GSH oxidation was conducted in positive-ion mode and revealed several products represented by ions with

m/z 307, 323, 350, 356, and 613 (Figure 7). The peak at m/z 308 corresponded to unmodified GSH. The ion with m/z 613 and the doubly charged ion with m/z 307 ($[M + 2H]^{2+}$) corresponded to the same molecule of GSSG. CID MS/MS spectrum of tripeptide glutathione was represented by the traditional b- and y-series of daughter ions. The spectrum of m/z 323 was consistent with the spectrum of glutathione in which oxygen was added to cysteine and, hence, represented glutathione sulfenic acid (GSOH) (Figure 8D,E). The m/z ratio for GSOH was 323, but not 324 as it should be, because of loss of the H from the OH group of the Cys residue during ionization. This loss was reproduced in the b- and y-series of GSOH daughter ions. Similarly, fragmentation spectrum of m/z

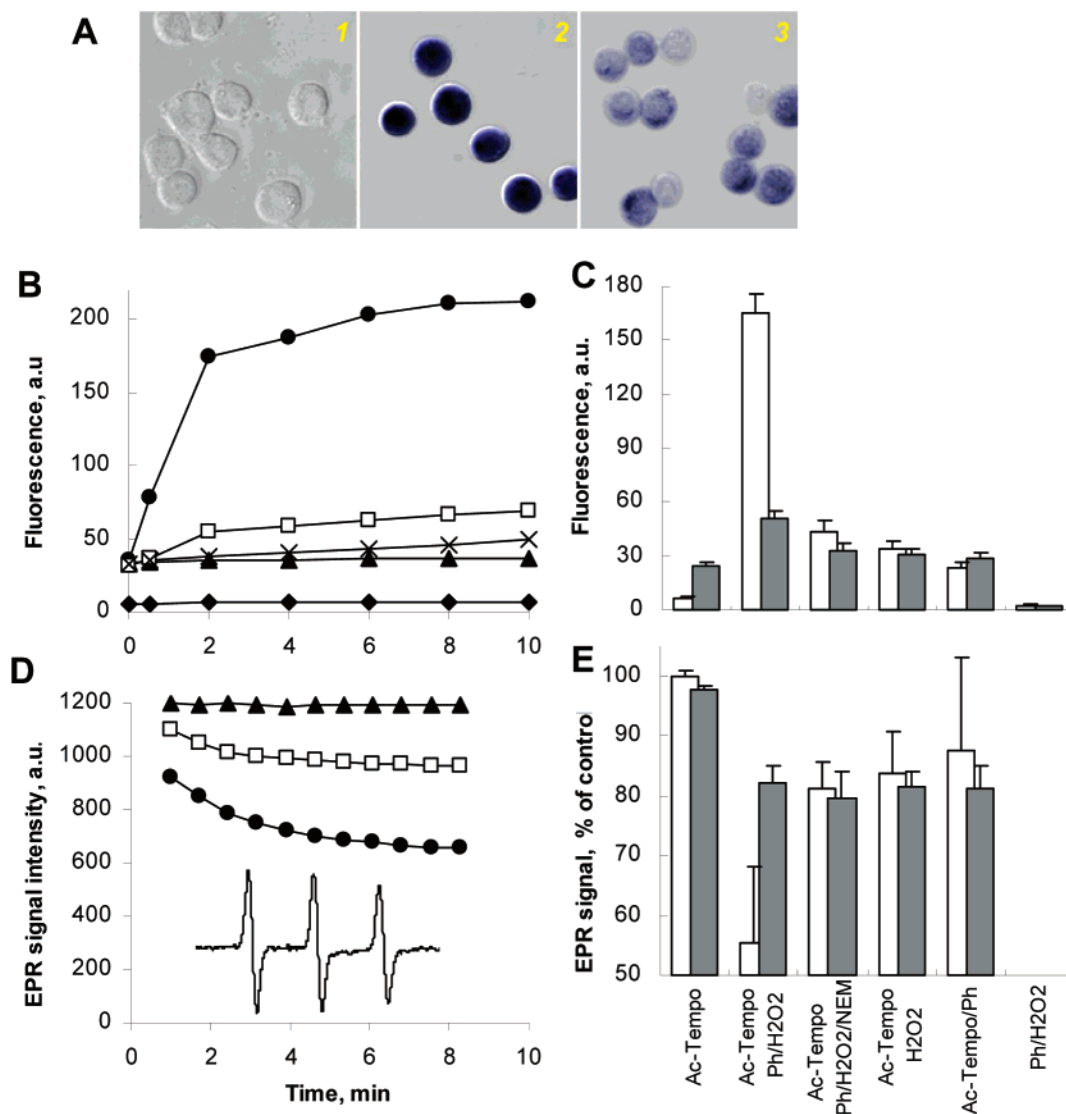


Figure 9. Interaction of Ac-Tempo with GSH and detection of glutathionyl radicals in HL-60 cells treated with phenol/H₂O₂. (A) Fluorescence images of cells were taken in 5 min after addition of reagents and then were overlaid on phase-contrast pictures of the same cells. (1) Ac-Tempo (20 μM). (2) Ac-Tempo plus phenol (100 μM) and H₂O₂ (20 μM). (3) Ac-Tempo plus phenol, H₂O₂, and NEM (50 μM). (B) Time course of Ac-Tempo fluorescence intensity: Ac-Tempo (10 μM) (▲); Ac-Tempo plus phenol, H₂O₂ (●); Ac-Tempo plus phenol, H₂O₂, and NEM (□); Ac-Tempo plus phenol, H₂O₂ and azide (2 mM) (×); phenol and H₂O₂ without Ac-Tempo (◆). Concentrations of reagents Ac-Tempo, phenol, H₂O₂, and NEM were the same as in (A), unless otherwise noted. (C) Total fluorescence from cells preincubated with or without SA for 48 h (gray and opened bars, respectively). Concentrations of reagents were the same as in (A). The legend is the same as that in (E). (D) Time course of EPR signals: Ac-Tempo (20 μM) (▲); Ac-Tempo plus phenol, H₂O₂ (●); Ac-Tempo plus phenol, H₂O₂, and NEM (□). Concentrations of reagents were the same as in (A). (E) Intensity of Ac-Tempo EPR signal at 15 min incubation from cells preincubated with or without SA for 48 h (gray and opened bars, respectively). All conditions are the same as in (A), with the exception of Ac-Tempo concentration (20 μM). Microscopy pictures and time course traces are representative recordings obtained from more than 5 experiments. Error bars represent SD obtained from at least three observations/point. At least 200 cells per experimental condition were evaluated to estimate average fluorescence by microscopy.

356 represented glutathione modified by three additional oxygen atoms on cysteine, and it corresponded to glutathione sulfonic acid (GSO₃H). A doubly charged ion with *m/z* 350 is described in the previous section. The relative intensities of peaks representing sulfenic and sulfonic acid changed from a prevalence of the sulfenic acid at the early stages of the peroxidase reaction to a predominance of the sulfonic acid by the end of the reaction.

Modification of Ac-Tempo Due to Peroxidase Activity in HL-60 Cells. HL-60 cells preincubated with Ac-Tempo were faintly visible by fluorescence microscopy (Figure 9A1). Addition of phenol or H₂O₂ to Ac-Tempo-treated cells induced fluorescence slightly; however, addition of phenol and H₂O₂ together to these cells caused a marked production of blue

fluorescence (Figure 9A2). Substantial inhibition of fluorescence (~80%) was observed in cells with depleted GSH (pretreated with NEM) (Figure 9A3). These data were corroborated by the measurements of fluorescence from cells in the suspension using spectrofluorometric assay (Figure 9B,C). In addition, fluorescence signals were also significantly quenched (~70%) in the cells, in which MPO activity was diminished by pretreatment with SA (Figure 9C).

Fluorescence responses were accompanied by the changes in the intensity of the Ac-Tempo EPR signal (Figure 9D,E). EPR signals were stable in the presence of cells unless phenol and H₂O₂ were added simultaneously, inducing decay of the intensity (Figure 9D,E). Pretreatment of cells with NEM or with SA prevented this decay (Figure 9E). In addition, both EPR

Table 1. Content of GSH and Protein SH-groups and Formation of Fluorescent Product from Ac-Tempo in HL-60 Cells Exposed to Phenol and H₂O₂^a

	protein SH ^b groups nmol/mln cells	GSH ^b nmol/mln cells	Ac-piperidine ^b nmol/mln cells	dead cells ^c %
phenol/Ac-Tempo	0.512 ± 0.069	0.439 ± 0.011	0.015 ± 0.003	6.8 ± 3.0
phenol/Ac-Tempo/H ₂ O ₂	0.498 ± 0.119	0.213 ± 0.003	0.247 ± 0.002	11.8 ± 4.0 ^d
phenol/H ₂ O ₂	0.403 ± 0.098	0.074 ± 0.018 ^d	N/A	24.5 ± 2.6
NEM/phenol/H ₂ O ₂	N/A	N/A	0.82 ± 0.009	N/A

^a Amount of intracellular fluorescent product formed from Ac-Tempo as determined by fluorescence spectrophotometry. Amount of GSH and protein SH groups in HL-60 cells was determined using the ThioGlo assay. Percentage of necrotic cells assessed by Trypan Blue exclusion. ^b Incubation conditions: 2 mL × 10⁹ cells/mL; 20 μM Ac-Tempo; 100 μM phenol; 200 μM H₂O₂; 15 min incubation time. ^c Incubation conditions: 100 μM Ac-Tempo; 100 μM phenol; 50 μM H₂O₂ were added 4 times (every 30 min during 2 h incubation period). ^d *p* < 0.05 versus cells treated with Ac-Tempo/phenol/H₂O₂. Data represent means ± SEM (*n* = 4).

and fluorescence responses were substantially reduced in the presence of peroxidase inhibitor, azide (Figure 9B,E).

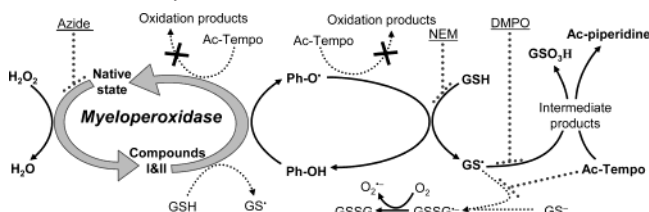
HPLC and MS analysis of the Ac-Tempo derivatives formed in cells and cell supernatant after H₂O₂ and phenol treatment has revealed that Ac-piperidine was the major (75–85%) product of the myeloperoxidase-dependent Ac-Tempo metabolism (data not shown).

Ac-Tempo Protects HL-60 Cells against Toxicity Caused by Phenol/H₂O₂. Treatment of HL-60 cells with phenol and H₂O₂ induced rapid oxidation of GSH (by 85%) as well as cell death, which was observable after 2 h of incubation (Table 1). Notably, protein SH groups were not affected by phenoxyl radical-dependent oxidation. In the presence of Ac-Tempo, the amount of GSH consumed in HL-60 cells (225 ± 11 pmol/10⁶ cells) was not statistically different from the amount of fluorescent Ac-piperidine produced (230 ± 4 pmol/10⁶ cells). Phenol caused greater GSH loss in the absence of Ac-Tempo (80% of total) than in its presence (50% of total). Decrease in cell viability during phenol/H₂O₂ exposure was also partially prevented by co-incubation with Ac-Tempo (Table 1), suggesting that Ac-Tempo protects HL-60 cells from phenol toxicity.

Discussion

Nontoxic nitroxides are considered as effective and promising antioxidants, and as a result, they have been extensively used to protect animals and cells from oxidative stress. Elucidation of nitroxide radical scavenging mechanisms is crucial for their optimized application. There is a lack of information regarding interactions of nitroxides with thiyl radicals, which are often involved in the oxidative stress-induced damage. In addition, pathways of deoxygenation of nitroxides in cells are unknown. Here, we demonstrated that nitroxides can effectively scavenge thiyl radicals in physiologically relevant conditions. This interaction is associated with the deoxygenation of nitroxide and, hence, may be considered as one of the primary nitroxide scavenging pathways of nitroxides in cells. Mechanism and significance of this reaction with respect to antioxidant function of nitroxides are discussed in the following paragraphs.

Reaction Mechanisms. GSH is not a good electron donor for peroxidases: rate constants for GSH oxidation by compounds I and II of MPO are 70 M⁻¹ s⁻¹ and <1 M⁻¹ s⁻¹, respectively.²⁰ On the other hand, phenols are good substrates. Peroxidases, such as HRP or MPO, contain phenol-binding sites and can readily oxidize phenolic compounds to corresponding phenoxyl radicals with rate constants of 10⁶ to 10⁸ M⁻¹ s⁻¹.²¹

Scheme 2. Interactions of Ac-Tempo during Peroxidase-Catalyzed Oxidation of Phenol and GSH^a

^a The major reaction pathways are represented by solid arrows.

Phenoxyl radicals are efficiently reduced back to phenol by GSH with concomitant formation of glutathionyl radicals.^{11,12}

We report here that paramagnetic and fluorescence properties of the nitroxide Ac-Tempo are dramatically changed during free-radical oxidation of GSH catalyzed by peroxidases in the presence of phenol. We assumed that glutathionyl radicals initiate the Ac-Tempo modification that causes loss of the nitroxide EPR signal and generation of acridine fluorescence (Scheme 2). Several suggestions could be made for the mechanism of the interaction between Ac-Tempo and GS•. GS• could react with the acridine moiety, with the acridine-Tempo peptide bond, or with the nitroxide moiety. In addition, the S-centered radical of glutathione could form, through intramolecular rearrangement, a C-centered radical that subsequently reacts with Ac-Tempo.

If the acridine moiety and acridine-Tempo peptide bond were involved in the reactions with GS•, unavoidable changes in the optical spectrum of the product, but not in its paramagnetic properties, should be observed. In our experiments, optical spectra were not significantly disturbed; rather, the paramagnetic properties of Ac-Tempo disappeared, supporting involvement of nitroxide moiety.

In addition, decay of the EPR signal and/or the appearance of fluorescence were observed upon incubation of various nitroxides (Ac-Tempo, PF, Tempo) with our peroxidase system and GSH. Similar changes, detected upon incubation of two thiols, GSH and cysteine, with Ac-Tempo, suggest that the thiol and nitroxide groups are the two reactive moieties. This nitroxide/GS• reaction was further corroborated by our MS and structural analyses that showed loss of nitroxide oxygen and formation of corresponding piperidine.

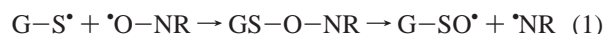
Formation of C-centered radicals can also be ruled out as a likely mechanism for several reasons. First, at physiological pH, intramolecular rearrangement has a relatively low rate (10³ s⁻¹),^{16b} which is inconsistent with our results showing fast modification of Ac-Tempo. Second, C-centered radicals form stable adducts with nitroxides;¹⁹ these adducts have not been

(20) Burner, U.; Obinger, C. *FEBS Lett.* **1997**, *411*, 269.

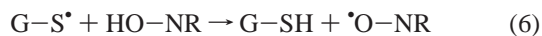
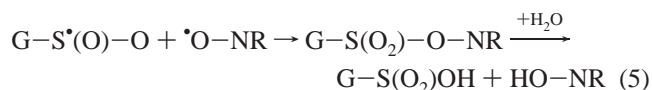
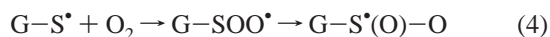
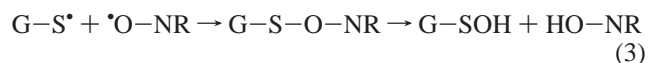
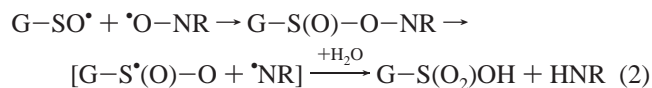
(21) Candeias, L. P.; Folkes, L. K.; Wardman, P. *Biochemistry* **1997**, *36*, 7081.

detected in our experiments. Third, cysteine, which presumably does not form C-centered radicals, was able to promote the same reaction with Ac-Tempo as GSH. Last, according to our MS results, the predominant products of GSH oxidation were sulfenic acid, sulfonic acid, and glutathione disulfide. Hence, all modifications of GSH took place at the sulfur moiety.

The most likely mechanism of the reaction is the formation of an intermediate of glutathione-nitroxide adduct, $-S-O-N<$, followed by cleavage of a relatively weak O-N bond leading to the formation of piperidine. Similar coupling reactions between Tempo and S-centered radicals derived from thiamine and thiophenols were reported previously in solid phase and in solution.¹³ Carloni et al. reported formation of thiophenol-nitroxide adducts and proposed a homolytic mechanism for the O-N bond cleavage in the thiol-nitroxide conjugate, with subsequent formation of aminyl and sulfinyl radicals (branching reaction):^{13b}



According to the equation, both radical products formed propagate free-radical oxidation of new nitroxide and thiol molecules leading to the formation of new radicals with consequent oxidation of thiols and consumption of nitroxides (branching and propagation reactions). Such a mechanism suggests dramatic enhancement of thiol oxidation in the presence of nitroxides. However, in our experiments, we did not observe any nitroxide-dependent increase of GSH oxidation, suggesting that multiple branching and propagation reactions did not take place. Furthermore, in contrast to reactions reported by Damiani et al. and Murayama et al., most products that would support such a reaction mechanism—various adducts between nitroxide and glutathione oxides—were not detected in our system. In addition, sulfonyl and sulfonyloxy radicals are relatively weak oxidants and can also act as reductants.²² Therefore, we propose an alternative list of reactions that would terminate, rather than propagate, the free-radical chain:



These reaction pathways explain the spectrum of detected products, including both sulfenic and sulfonic acids as well as

Ac-piperidine, Ac-Tempo-H, and Ac-Tempo-glutathione sulfoxide adducts. A prevalence of these reactions could also exclude propagation of GSH oxidation. However, this does not exclude the existence of other mechanisms, including heterolytic decomposition of $GS-O-NR$, with a very different cascade of subsequent events or even coexistence of different mechanisms in the same reaction system.

We report that piperidine and pyrrolidin nitroxides irreversibly react with cysteine and glutathione thiyl radicals generated both by photodecomposition of $GS-NO$ and by the peroxidase-dependent system. Major end products formed from nitroxide and thiol are secondary amines and sulfonic acid, respectively. This reaction appears to be very efficient, since the yield of end products is around 80–90%. On the basis of the results of our inhibition experiments with various GSH concentrations as well as on known rate constants for primary reactions of GS^{\bullet} and its derivatives ($GSSG^{\bullet-}$, $GSOO^{\bullet}$)^{9b,16} and use of computer modeling, we estimated the reaction rate of GS^{\bullet} with Ac-Tempo to be near $10^8 M^{-1} s^{-1}$. A similar rate constant was also derived from our competition experiments with DMPO; the latter reacts with GS^{\bullet} at a rate of $\sim 10^6$ to $10^7 M^{-1} s^{-1}$ as previously reported and as estimated in our computer modeling.²³ On the basis of these values, reaction rate of GS^{\bullet} with Ac-Tempo will be in the range 10^8 to $10^9 M^{-1} s^{-1}$. These estimated values using our experimental results correspond to the rate constant previously reported for the reactions of Tempo with phenylsulfenyl (thiyl) and phenylsulfinyl radicals ($\sim 10^9 M^{-1} s^{-1}$).²⁴

Role of Nitroxides in Cell Protection against Thiyl Radicals. On the basis of the interaction of nitroxide with thiyl radicals in the peroxidase system, we applied Ac-Tempo for the detection and imaging of myeloperoxidase-induced thiyl radicals in HL-60 cells. Overall, data from HL-60 cell experiments correlated well with our data from the model peroxidase system: in cells, conversion of nitroxide to piperidine was promoted by myeloperoxidase, and generation of thiyl radicals accounted for the appearance of intracellular fluorescence. Strong fluorescence responses were observed only under conditions favorable for thiyl radical formation; generation of fluorescence correlated well with consumption of GSH. Depletion of either intracellular thiols or myeloperoxidase resulted in significant inhibition of fluorescence production. It is still possible that a small fraction of hyper-reactive SH groups of proteins can also participate in interactions of nitroxides with intracellular thiols. Furthermore, HPLC and MS analysis revealed that Ac-piperidine was the major product of MPO-dependent Ac-Tempo metabolism in cells.

As has been demonstrated previously, secondary amine is the major product of nitroxide metabolism in cells. However, which biochemical pathway leads to the formation of this product is not known.⁵ We suggest that interaction of nitroxide with cysteine and glutathione thiyl radicals is the biologically relevant reaction responsible for the deoxygenation of nitroxide. This reaction could also contribute to the protective properties of nitroxides, since it efficiently removes thiyl radicals. Indeed, in our experiments Ac-Tempo significantly prevented phenol/ H_2O_2 -induced oxidation of GSH and protected against cytotoxic effect of phenol/ H_2O_2 . Taking into consideration that, in

(22) (a) Bahnmann, D. Photocatalytic formation of sulfur-centered radicals by one-electron redox processes on semiconductor surfaces. In *Sulfur-Centered Reactive Intermediates in Chemistry and Biology*; Proceedings of NATO ASI, Maratea, Italy, June 18–30, 1989; Chatgililoglu, C., Asmus K. D., Eds.; Plenum Press: New York, 1989; Vol. 197, pp 103–120. (b) Minisci, F. The invention of radical chain reactions of value in organic chemistry. In *Sulfur-Centered Reactive Intermediates in Chemistry and Biology*; Proceedings of NATO ASI, Maratea, Italy, June 18–30, 1989; Chatgililoglu, C., Asmus K. D., Eds.; Plenum Press: New York, 1989; Vol. 197, pp 303–317.

(23) Karoui, H.; Hogg, N.; Frejaville, C.; Tordo, P.; Kalyanaraman, B. *J. Biol. Chem.* **1996**, *271*, 6000.

(24) Darmanyan, A. P.; Gregory, D. D.; Guo, Y. S.; Jenks, W. S. *J. Phys. Chem. A* **1997**, *101*, 6855.

peroxidase-rich cells, this pathway of GSH oxidation occurs mainly through a free-radical mechanism and that Ac-Tempo efficiently reacted with thiyl radicals, we assumed that interaction of thiyl radicals is the reaction that mediates the beneficial effect of nitroxides. Interestingly, the thiyl radical reaction with nitroxide could also contribute to the protective function of the nitron spin trap, PBN, which has been widely implicated as an antioxidant *in vivo*.²⁵ A traditional explanation for the protective effects of PBN against ionizing radiation, during ischemia/reperfusion, and traumatic brain injury is its scavenging activity toward ROS.²⁵ However, free-radical reactions of PBN nitron yield its nitroxide, which appears not only to exert substantial ability to quench thiyl radicals but also could account for PBN's antioxidant role.

On the basis of the thiyl radical-nitroxide interactions described here, particularly those observed in peroxidase-dependent myeloid cells, nitroxide could be targeted for use in medical conditions associated with thiyl radical production. Peroxidases and heme proteins with peroxidase activity are involved in numerous aspects of cell and organism physiology. Myeloperoxidase is central to host defense systems, producing highly toxic HOCl for microorganisms; cyclooxygenase catalyzes synthesis of prostaglandins, important regulators of inflammatory response and vascular tone; and cytochrome *c*, which shuttles electrons through the electron transport chain in

(25) Lee, J. H.; Park, J. W. *Cancer Res.* **2003**, *63*, 6885.

mitochondria, may act as a peroxidase in redox signaling during apoptosis.²⁶ In the presence of phenolic compounds, peroxidases generate phenoxyl radicals that dramatically facilitate oxidation of GSH to thiyl radicals. As potent oxidants, the latter can attack critical biomolecules and cause cell damage. For example, commonly used phenolic drugs (such as acetaminophen and etoposide) and numerous environmental phenolic compounds can induce cell damage by redirecting H₂O₂ metabolism from a "safe", nonradical pathway controlled by non-heme GSH peroxidase to a free-radical pathway orchestrated by heme-containing peroxidases. Presumably, nitroxides, which, as shown here, are able to scavenge GS•, could be used to develop protective strategies for reducing side effects of phenolic compounds in peroxidase-rich cells. In addition, conjugates of nitroxides with fluorogenic molecules can be used for detection and imaging of thiyl radical production in live cells.

Acknowledgment. This work was supported by NIH Grants HL70755, HL64145, and the International Neurological Science Fellowship Program (F05 NS43922-02) administered by NIH/NINDS in collaboration with WHO. We thank Dr. T. Bradley for her help in preparing the manuscript.

JA0495157

(26) (a) Rosen, H.; Crowley, J. R.; Heinecke, J. W. *J. Biol. Chem.* **2002**, *277*, 30463. (b) Minghetti, L.; Levi, G. *Prog. Neurobiol.* **1998**, *54*, 99. (c) Jiang, J. F.; Serinkan, B. F.; Tyurina, Y. Y.; Borisenko, G. G.; Mi, Z. B.; Robbins, P. D.; Schroit, A. J.; Kagan, V. E. *Free Radical Biol. Med.* **2003**, *35*, 814.